THE JOURNAL OF PHYSICAL CHEMISTRY Letters

Letter

Cite This: J. Phys. Chem. Lett. 2019, 10, 4596−4602

pubs.acs.org/JPCL

Tailoring the Photoluminescence Excitation Dependence of the Carbon Dots via an Alkali Treatment

Yun Yang Zhao,[†] Song Nan Qu,[†] Xi Yuan Feng,[†] Jin Cheng Xu,[†] Ye Yang,[†] Shi Chen Su,[‡] Shuang Peng Wang,*[,†] and Kar Wei Ng*[,†]

[†]Joint Key Laboratory of the Ministry of Education, Institute of Applied Physics and Materials Engineering, University of Macau, Avenida da Universidade, Taipa, Macao SAR, China

[‡]Institute of Optoelectronic Material and Technology, South China Normal University, Guangzhou 510631, People's Republic of China

Supporting Information

ABSTRACT: Carbon dots (CDs) have shown great potential in various applications including biomedicines and optoelectronics. However, the origin of their photoluminescence excitation dependence (PL-ED) still remains uncertain, and this can limit the full exploit of their wonderful optical properties. Here we studied the mechanism for the PL-ED of solvothermally synthesized CDs using an alkali treatment. As-synthesized CDs were found to agglomerate and exhibited multicolor emissions with strong PL-ED. The alkali treatment can effectively break down the clusters into individual CDs via the hydrolysis of the amide and ester bonds that link the CDs together. This process effectively narrowed the emission line width and suppressed the observed PL-ED. The understanding of the excitation dependence mechanism here outlined a novel strategy for tailoring of the PL-ED of CDs via a synergy of chemical and physical processes, thus enhancing the versatility of CDs for a broader spectrum of applications.

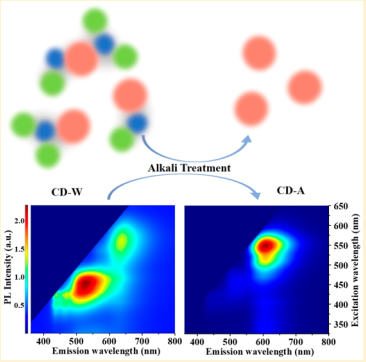

As an emerging carbon nanomaterial, carbon dots (CDs) have attracted much attention due to their numerous advantages including low cost, low toxicity, and good biocompatibility. These attractive properties render them potentially useful in optoelectronics,[1−4] biomedicines,[5−8] and many other applications.[9−14] In general, CDs can be synthesized either by top-down approaches like chemical oxidation, which cuts bulk carbon materials into nanosized CDs,[15,16] or via the bottom-up dehydration and graphitization of simple organic molecules.[17,18] Interestingly, the photoluminescence (PL) of these synthesized CDs usually shows different degrees of excitation dependence, i.e., the sensitivity of the peak emission wavelength toward the excitation wavelength. While some studies suggest that such dependence originates from the presence of multiple surface active sites on individual CDs,[19] other researchers report that the mixing of CDs with different sizes and thus emission wavelengths contributes to the observed excitation dependence.[18,20−23] The exact mechanism of such dependence is highly correlated with the synthesis method as well as the surface treatment.[22,24,25] Among all of the bottom-up techniques, solvo/hydrothermal processes have shown great promise in realizing functional CDs with extraordinary optical performances.[6,26,27] While excitation dependence is also observed in CDs synthesized with this method, the origin of such a phenomenon still remains unclear. To flexibly tailor the emission properties of these CDs for different applications, a comprehensive study to fully understand the root cause of this photoluminescence excitation dependence (PL-ED) is therefore mandatory.

In this Letter, we investigate the origin of the PL-ED of solvothermally synthesized CDs using an alkali treatment. As-synthesized CDs exhibit multicolor emissions whose relative intensities show strong dependence on the excitation wavelengths. After the alkali treatment, however, such dependence has been remarkably suppressed and the CDs emit predominantly at around 630 nm under all excitation wavelengths. Using various characterization techniques, we discovered that the PL-ED of as-synthesized CDs originates from the clustering of CDs with various degrees of graphitization. Notably, these CDs are connected with amorphous structures composed mainly of ester and amide bonds and thus cannot be separated solely by physical means. The alkali effectively facilitates the hydrolysis of these bonds, leading to the isolation of CDs with surfaces stabilized with amino, hydroxyl, and carboxyl groups. The subsequent centrifugation process further separates CDs with larger size and thus higher graphitization from the mixture, resulting in the observed suppression of PL-ED. The understanding of the PL-ED mechanism here outlined a novel strategy to tailor the excitation dependence of CDs via a synergy of chemical and

Received: June 26, 2019
Accepted: July 30, 2019
Published: July 30, 2019

DOI: 10.1021/acs.jpclett.9b01848
J. Phys. Chem. Lett. 2019, 10, 4596−4602

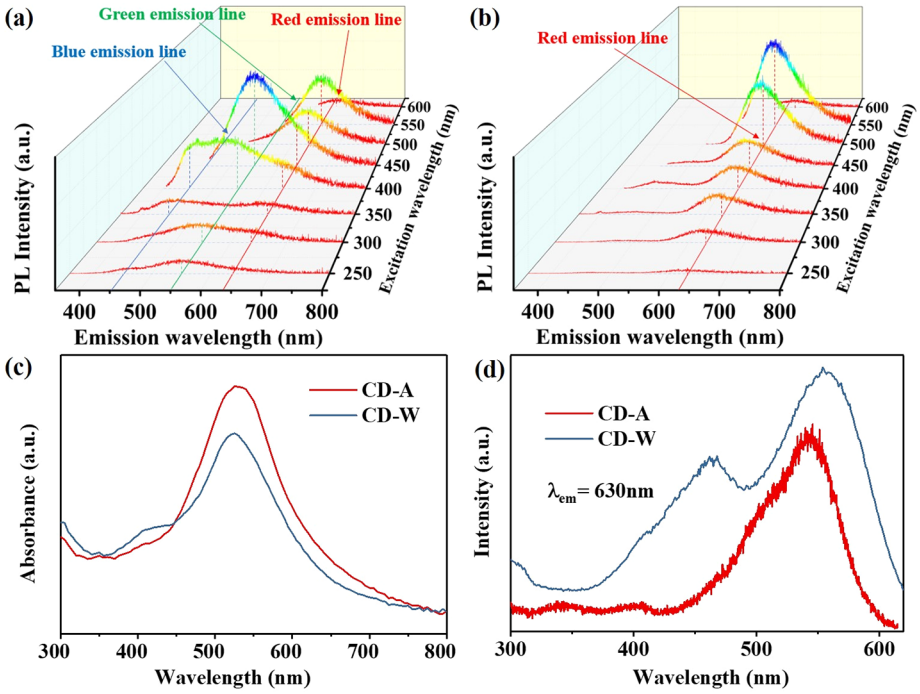

Figure 1. PL spectra of (a) CD-W, which shows multicolor emission with high PL-ED, and (b) CD-A, which gives red emission with suppressed PL-ED under various excitation wavelengths. (c) Absorption spectra and (d) PLE spectra of CD-W and CD-A.

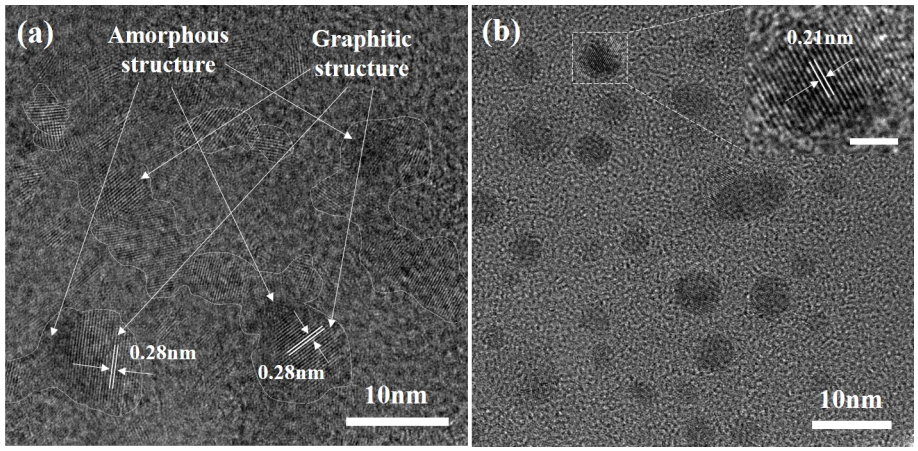

Figure 2. HRTEM of (a) CD-W and (b) CD-A. As-synthesized CDs in (a) exist as clusters in which the CDs are linked together by amorphous structures (outlined with dashed lines). After the alkali treatment, the clusters are isolated into individual CDs. The inset shows an enlarged HRTEM image of one CD with a scale bar of 2 nm.

physical processes, thus enhancing the versatility of CDs for broader applications.

The CDs in this work were synthesized with a solvothermal method.[20,21] Typically, 2 g of citric acid and 4 g of urea were dissolved into 20 mL of *N*,*N*-dimethylformamide. The mixture solution was then transferred into a 50 mL Teflon-lined stainless-steel autoclave and heated at 160 °C for 4 h. After cooling down to room temperature, the mixture solution was centrifuged at 18500 rpm for 20 min to extract the CDs. The extract was then divided into two halves: the first half was washed with water to obtain CD-W; the other half was dipped into a 20 mL NaOH solution and further centrifuged. The precipitate and the remaining materials in the supernatant were then neutralized with HCl and washed with water to obtain CD-A and CD-S, respectively. Details of the synthesis and characterizations can be found in the Supporting Information.

The alkali treatment exerts a significant impact on the PL-ED of the CDs. As displayed in Figure 1a, CD-W gives a broad PL emission spectrum with three dominant peaks at ∼450 (blue), 550 (green), and 630 nm (red). Notably, the intensities of these emissions display strong dependences on the excitation wavelength (λ_{ex}). At $\lambda_{ex} \leq 400$ nm, CD-W exhibits very weak emissions due to the low absorption and thus inefficient excitation at the ultraviolet regime, as shown in Figures 1c,d and S1a. The blue and green emissions become dominant when λ_{ex} goes into the visible light regime. The two emissions are of similar intensities at $\lambda_{ex} = 400$ nm, followed by dominance of the green emission at $\lambda_{ex} = 450$ nm. At $\lambda_{ex} > 500$ nm, the pumping light can no longer effectively excite the green emission peak, and the red emission becomes the sole dominant peak. Such behavior attests to the strong PL-ED of CD-W. In sharp contrast, the PL of CD-A in Figure 1b is

DOI: 10.1021/acs.jpclett.9b01848
J. Phys. Chem. Lett. 2019, 10, 4596−4602

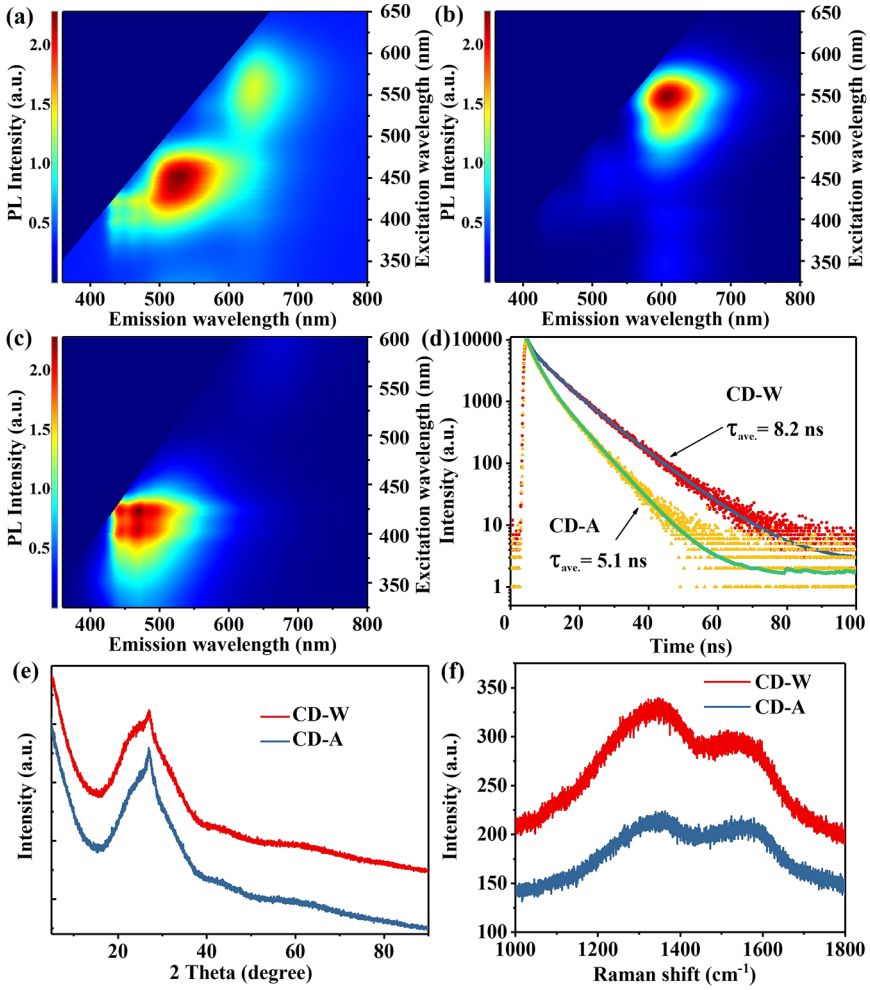

Figure 3. EEMs of (a) CD-W, (b) CD-A, and (c) CD-S. The emission area in the top left corner is automatically deleted by the instrument due to the Rayleigh scattering, which is similar to the previous work.[17] (d) TRPL decay curves of CD-W and CD-A; the red and yellow scattered dots are the raw TRPL decay data of CD-W and CD-A, respectively, and fitted with a tri- and biexponential decay function (dark blue and green curves) to obtain the average carrier lifetime ($\tau_{ave.}$) of CD-W and CD-A, respectively. (e) XRD pattern and (f) Raman spectra of CD-W and CD-A, which indicates the enhanced graphitization of the CDs after alkali treatment.

always dominant with the red emission at all λ_{ex}. The absence of the blue and green emissions in CD-A signifies the deactivation or removal of the blue- and green-emitting structures after the alkali treatment. Such a hypothesis can be further substantiated with the absorption spectra and photoluminescent excitation (PLE) spectra of the two samples. Compared with CD-W, the absorption peak at around 420 nm diminishes in CD-A (see Figure 1c), indicating that the absorber for violet light, likely the blue emitters in CD-W, has been removed during the alkali treatment. In addition, from the PLE spectra taken at an emission wavelength of 630 nm in Figure 1d, one can observe that red emission in CD-A is most effectively excited by λ_{ex} close to 550 nm. The PLE of CD-W, however, shows an additional peak at around 460 nm, indicating the presence of a structure that can effectively absorb blue light and transfer the energy for red emissions. Details of this energy transfer process will be discussed shortly. The results here indicate that the PL-ED of as-synthesized CDs, i.e., CD-W, may originate from the presence of multicolor emitters, which can be deactivated or removed by the alkali treatment, thus completely transforming the emission properties of the CDs.

High-resolution transmission electron microscopy (HRTEM) was utilized to study the possible structural changes in the CDs leading to the transformation in optical properties. As displayed in Figures 2a and S2a–f, the nanostructures in CD-W exist as clusters of randomly oriented graphitic dots with well-resolved lattice fringes. Most of them have irregular shapes and sizes and are surrounded by amorphous structures that can only be subtly distinguished in the TEM images. Notably, the existence of an amorphous layer wrapping around the graphitic structures is also observed in other previous works.[27,28] We believe that the CDs are firmly connected by these amorphous structures and thus cannot be separated physically by centrifugation in water. The agglomeration of CDs with various sizes and surface conditions is possibly the cause for the observed multicolor emissions and PL-ED. On the contrary, well-isolated CDs with elliptical or circular shapes are observed in CD-A in Figures 2b and S2g–l. While the amorphous structures linking the CDs together no longer exist, the graphitic structure is well preserved after the treatment (see the inset of Figure 2b). Indeed, we observed that the CDs in CD-A are larger in size than CD-S in Figure S5. These observations suggest that NaOH can effectively break the amorphous links, thus converting the clusters into

DOI: 10.1021/acs.jpclett.9b01848
J. Phys. Chem. Lett. 2019, 10, 4596–4602

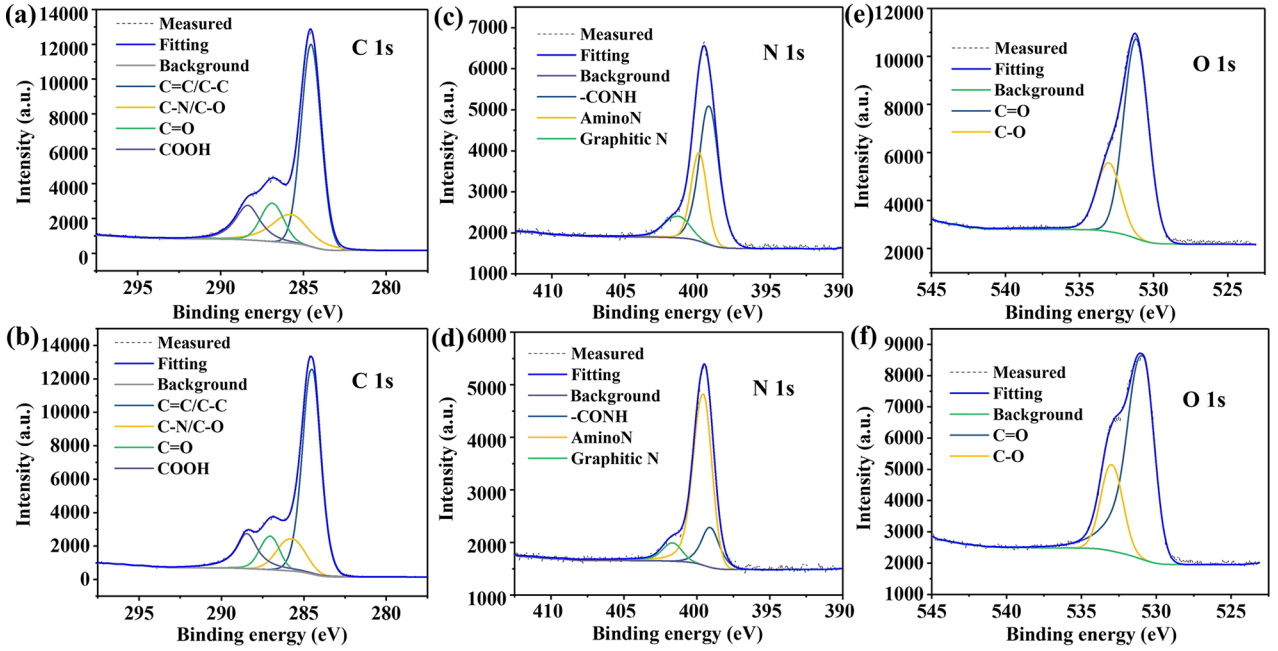

Figure 4. High-resolution C 1s, N 1s, and O 1s XPS spectra of CD-W (a,c,e) and CD-A (b,d,f).

isolated CDs that exhibit completely different emission properties from the agglomerate.

To further verify the correlation between clustering and the observed luminescence properties of the CDs, we studied the detailed PL-ED via excitation−emission maps (EEMs). As shown in Figure 3a, the emission of CD-W shows a strong dependence on λ_{ex} and covers a wide spectrum ranging from blue to red light, which is consistent with Figure 1a. Notably, such multicolor emission is still well preserved in CD-W even after multiple extra cycles of centrifugation in water. The EEMs of the products after treatments are displayed in Figure 3b,c. While the EEM of CD-A is dominated solely by red emission under all λ_{ex}, CD-S shows a relatively broad emission over the blue and green regimes, as shown in Figure 3c. Indeed, we observed that the CDs in CD-A are larger in size than those in CD-S in Figure S5. These observations indicate that the alkali treatment can effectively separate the red CDs from the CD clusters in CD-W. Such an isolation process is further confirmed with time-resolved photoluminescence (TRPL). As seen in the TRPL decay curves in Figure 3d, the average carrier lifetime of CD-W is 60% longer than that of CD-A. In addition, while the decay curve of CD-W is best fitted with a triexponential function, that of CD-A shows a biexponential behavior, indicating that an extra process occurs in the red emission from CD-W. We attribute the additional step to energy transfer from the green and blue CDs to the neighboring red ones in the clusters, thus resulting in the observed longer carrier lifetime and triexponential decay process in CD-W. Such energy transfer, via either the absorption of high-energy photons by small-bandgap CDs or nonradiative resonance transfer, can only effectively occur at short distance. The disappearance of this energy transfer step clearly reveals that the CDs are separated far apart during the alkali treatment. The detailed studies in EEMs and emission transient behaviors clearly exemplify that the alkaline treatment can effectively decluster and isolate the as-synthesized CDs, thus resulting in the observed change in PL-ED.

Interestingly, the green emissions are rather weak in the EEMs of CD-A and CD-S under all λ_{ex}. One possible reason is the dilution of the green CDs over CD-A and CD-S during the centrifugation process. Another possible reason is the suppression of energy transfer from blue to green CDs because the alkali treatment isolates the CDs far apart. A more detailed discussion can be found in the Supporting Information.

In addition to understanding the origin of the PL-ED, it is crucial to investigate the reaction mechanisms involved in separating the clustered CDs during the alkali treatment. We first studied the change in graphitization level of the CDs using X-ray diffraction (XRD) and Raman spectroscopy. Figure 3e shows the XRD patterns of CD-A and CD-W. Both curves consist of a sharp peak overlapping with a broad diffraction at around 25°. While the sharp peak centered at 26.6° corresponds to the 002 diffraction of the graphitic structure,[2,29] the broad peak can be attributed to amorphous structures with low crystallinity.[30,31] The increased intensity ratio between the sharp and broad diffractions implies an enhancement in graphitization after treatments. Such observation is consistent with the results obtained from Raman spectroscopy, as displayed in Figure 3f. The D band (1350 cm^{-1}) and G band (1580 cm^{-1}) stand for the vibrations from amorphous and graphitic carbon of CDs, respectively. The intensity ratio of the two bands (I_D/I_G) decreases from 1.14 to 1.04 after the alkali treatment, confirming the rise of the graphitization level after treatment. With the graphitic structure of the CDs well preserved (as observed in TEM), the enhanced overall graphitization of CDs after the NaOH dip suggests that the amorphous structures connecting the CDs, usually composed of sp^3 carbons, were removed during the process, thus leading to the observed isolation of the CDs.

X-ray photoelectron spectroscopy (XPS) was employed to study how NaOH interacts with the amorphous structures. Figure S3 shows the XPS full survey spectra of CD-W and CD-A. Three main peaks originating from carbon, nitrogen, and oxygen can be clearly observed. The atomic composition of each element is shown in Table S1. Notably, the ratio of C to

DOI: 10.1021/acs.jpclett.9b01848
J. Phys. Chem. Lett. 2019, 10, 4596−4602

Scheme 1. Possible Evolution Process for CD-W and CD-A[a]

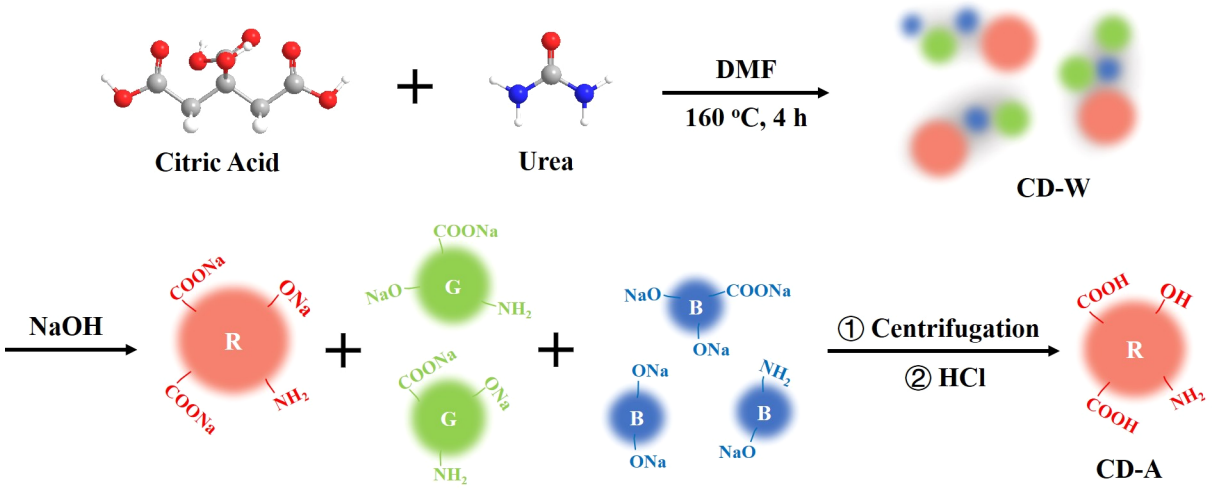

[a]R, G, and B stand for red, green, and blue emissive CDs. The surface functional groups on the CDs are arbitrarily assigned to illustrate the random nature of the CD synthesis process.

O is approximately 3.5:1 in both CD-W and CD-A, which is considerably higher than that in citric acid and urea due to the dehydration and carbonization of the precursors during CD formation. In addition, a significant drop in N content is observed after the treatments, suggesting that the amorphous structures connecting the CDs in the cluster are nitrogen rich. Figure 4a,b shows the high-resolution XPS spectra of C 1s, which were fitted into four kinds of C species: graphitic carbon (C═C/C−C), carbon single bonds like C−O/C−N, −C═O, and −COOH located at 284.5, 285.7, 287.1, and 288.5 eV, respectively.[21] The corresponding content of each C species is summarized in Table S2. The proportion of sp^2 carbon domain increases by over 3% after the treatments, confirming once again the enhanced graphitization in CD-A as observed in the XRD and Raman spectroscopy. To further understand the reaction mechanism involved in the declustering process, we carefully examine the high-resolution XPS spectra of N 1s and O 1s displayed in Figure 4c−f. While N exists predominantly as amides in CD-W, the largest proportion of N exists in amino groups in CD-A (see Table S3). In addition, an increase in the content of C−O can be observed from the O 1s spectrum after the post-treatments (see Table S4), which is likely correlated with the rise in −COOH contents in the C 1s spectrum (see Figure 4a,b and Table S1).[21,32] Detailed Fourier transform infrared (FTIR) spectra of these CDs and the high-resolution XPS of CD-S were also investigated and given in the Supporting Information (Figures S3 and S4). From these observations, we can deduce that the CDs in CD-W are connected together with amorphous carbon structures composed mainly of interlinking amide and ester bonds. Upon exposure to NaOH, these bonds undergo hydrolysis to form carboxyl, hydroxyl, and amino groups which terminate on the CD surface, resulting in the release of surface-stabilized individual CDs from the interconnected clusters.

With all the experimental results, we derived a possible reaction pathway, as shown in Scheme 1. Citric acid and urea went through dehydration, polymerization, carbonization, nucleation, and core−shell growth to form CDs with various sizes and thus emission wavelengths.[6,17,18] When multiple CDs nucleate close to one another, cross-linking may occur, resulting in cluster-like structures in CD-W. Notably, the CDs are connected to one another via amide and ester bonds, which cannot be broken solely by washing with water physically. NaOH acts as chemical scissors, which cut these bonds by hydrolysis and isolate the CDs with surfaces mainly terminated with amino groups, sodium carboxylates, and sodium hydroxylates. In the subsequent centrifugation process, most of the green and blue CDs and the amorphous linking structures are separated from the red CDs, leading to the enhancement of graphitization and the pure red emission in CD-A. During these processes, the roles of NaOH are (1) to provide an alkaline environment and facilitate the hydrolysis of ester and amide bonds; (2) to enrich the amount of carboxyl, hydroxyl and amino groups of CDs; and (3) to act as chemical scissors to cut off some amorphous carbon and polish the surface of CDs.[33] The roles of HCl are (1) to neutralize the excess alkali in the solution and (2) to exchange Na^+ from the surface of CDs with H^+. Scheme 1 clearly illustrates that the post-treatments can isolate the clustered CDs and completely modify the optical properties of the CDs by eliminating the energy transfer and PL-ED.

In summary, we presented a comprehensive study to show that clustering of CDs with various emission wavelengths can be a major cause for the PL-ED observed in solvothermally synthesized CDs. The CDs were found to be connecting with amorphous structures and thus could not be separated only by physical means. Using a facile alkali treatment, we demonstrated the breakdown of the clusters into individual CDs chemically by promoting the hydrolysis of the interconnecting amide and ester bonds. The structural change induced by the alkali treatment leads to transformation of the optical properties of the CDs, especially in terms of PL-ED. Our understanding here opened a possible pathway for the flexible tailoring of the PL-ED of the synthesized CDs via a series of chemical and physical processes, which can be useful in engineering the emission properties of CDs for various applications.

DOI: 10.1021/acs.jpclett.9b01848
J. Phys. Chem. Lett. 2019, 10, 4596−4602

■ ASSOCIATED CONTENT

Supporting Information

The Supporting Information is available free of charge on the ACS Publications website at DOI: 10.1021/acs.jpclett.9b01848.

Detailed experimental section, detailed discussion on the EEMs, and Figures S1−S6 and Tables S1−S6, including more detailed structural analysis of CD-S (PDF)

Brief synthesis process and structural transformation of the CDs as well as the interaction among the CDs before and after the alkali treatment (MP4)

■ AUTHOR INFORMATION

Corresponding Authors

*E-mail: billyng@um.edu.mo.

*E-mail: spwang@um.edu.mo.

ORCID

Yun Yang Zhao: 0000-0001-8955-6918

Shuang Peng Wang: 0000-0001-8464-4994

Kar Wei Ng: 0000-0002-6047-3104

Notes

The authors declare no competing financial interest.

■ ACKNOWLEDGMENTS

This work was funded by the Science and Technology Development Fund, Macau SAR (File No. 084/2016/A2, 051/2017/A, 199/2017/A3, and 0125/2018/A3) and Multi-Year Research Grants (MYRG2017-00152-FST, MYRG2017-00149-FST, SRG2016-00085-FST, and MYRG2018-00086-IAPME) from the Research & Development Office at the University of Macau.

■ REFERENCES

(1) Yuan, F.; Wang, Z.; Li, X.; Li, Y.; Tan, Z. a.; Fan, L.; Yang, S. Bright Multicolor Bandgap Fluorescent Carbon Quantum Dots for Electroluminescent Light-Emitting Diodes. *Adv. Mater.* **2017**, *29*, 1604436.

(2) Wang, Z.; Yuan, F.; Li, X.; Li, Y.; Zhong, H.; Fan, L.; Yang, S. 53% Efficient Red Emissive Carbon Quantum Dots for High Color Rendering and Stable Warm White-Light-Emitting Diodes. *Adv. Mater.* **2017**, *29*, 1702910.

(3) Li, X.; Rui, M.; Song, J.; Shen, Z.; Zeng, H. Carbon and Graphene Quantum Dots for Optoelectronic and Energy Devices: A Review. *Adv. Funct. Mater.* **2015**, *25*, 4929−4947.

(4) Zhang, T.; Zhao, F.; Li, L.; Qi, B.; Zhu, D.; Lü, J.; Lü, C. Tricolor White-Light-Emitting Carbon Dots with Multiple-Cores@Shell Structure for WLED Application. *ACS Appl. Mater. Interfaces* **2018**, *10*, 19796−19805.

(5) Li, D.; Jing, P.; Sun, L.; An, Y.; Shan, X.; Lu, X.; Zhou, D.; Han, D.; Shen, D.; Zhai, Y.; Qu, S.; Zbořil, R.; Rogach, A. L. Near-Infrared Excitation/Emission and Multiphoton-Induced Fluorescence of Carbon Dots. *Adv. Mater.* **2018**, *30*, 1705913.

(6) Ding, H.; Wei, J.-S.; Zhang, P.; Zhou, Z.-Y.; Gao, Q.-Y.; Xiong, H.-M. Solvent-Controlled Synthesis of Highly Luminescent Carbon Dots with a Wide Color Gamut and Narrowed Emission Peak Widths. *Small* **2018**, *14*, 1800612.

(7) Yao, H.; Zhao, W.; Zhang, S.; Guo, X.; Li, Y.; Du, B. Dual-Functional Carbon Dot-Labeled Heavy-Chain Ferritin for Self-Targeting Bio-Imaging and Chemo-Photodynamic Therapy. *J. Mater. Chem. B* **2018**, *6*, 3107−3115.

(8) Zeng, Q.; Shao, D.; He, X.; Ren, Z.; Ji, W.; Shan, C.; Qu, S.; Li, J.; Chen, L.; Li, Q. Carbon Dots as a Trackable Drug Delivery Carrier for Localized Cancer Therapy in Vivo. *J. Mater. Chem. B* **2016**, *4*, 5119−5126.

(9) Liu, Y.; Wu, P. Graphene Quantum Dot Hybrids as Efficient Metal-Free Electrocatalyst for the Oxygen Reduction Reaction. *ACS Appl. Mater. Interfaces* **2013**, *5*, 3362−3369.

(10) Bhattacharyya, S.; Konkena, B.; Jayaramulu, K.; Schuhmann, W.; Maji, T. K. Synthesis of Nano-Porous Carbon and Nitrogen Doped Carbon Dots From an Anionic MOF: a Trace Cobalt Metal Residue in Carbon Dots Promotes Electrocatalytic ORR Activity. *J. Mater. Chem. A* **2017**, *5*, 13573−13580.

(11) Wang, R.; Lu, K.-Q.; Tang, Z.-R.; Xu, Y.-J. Recent Progress in Carbon Quantum Dots: Synthesis, Properties and Applications in Photocatalysis. *J. Mater. Chem. A* **2017**, *5*, 3717−3734.

(12) Qu, S.; Liu, X.; Guo, X.; Chu, M.; Zhang, L.; Shen, D. Amplified Spontaneous Green Emission and Lasing Emission From Carbon Nanoparticles. *Adv. Funct. Mater.* **2014**, *24*, 2689−2695.

(13) Jiang, K.; Wang, Y.; Cai, C.; Lin, H. Conversion of Carbon Dots from Fluorescence to Ultralong Room-Temperature Phosphorescence by Heating for Security Applications. *Adv. Mater.* **2018**, *30*, 1800783.

(14) Qu, S.; Wang, X.; Lu, Q.; Liu, X.; Wang, L. A Biocompatible Fluorescent Ink Based on Water-Soluble Luminescent Carbon Nanodots. *Angew. Chem., Int. Ed.* **2012**, *51*, 12215−12218.

(15) Hu, C.; Yu, C.; Li, M.; Wang, X.; Yang, J.; Zhao, Z.; Eychmüller, A.; Sun, Y.-P.; Qiu, J. Chemically Tailoring Coal to Fluorescent Carbon Dots with Tuned Size and Their Capacity for Cu(II) Detection. *Small* **2014**, *10*, 4926−4933.

(16) Jing, S.; Zhao, Y.; Sun, R.-C.; Zhong, L.; Peng, X. Facile and High-Yield Synthesis of Carbon Quantum Dots from Biomass-Derived Carbons at Mild Condition. *ACS Sustainable Chem. Eng.* **2019**, *7*, 7833−7843.

(17) Shamsipur, M.; Barati, A.; Taherpour, A. A.; Jamshidi, M. Resolving the Multiple Emission Centers in Carbon Dots: From Fluorophore Molecular States to Aromatic Domain States and Carbon-Core States. *J. Phys. Chem. Lett.* **2018**, *9*, 4189−4198.

(18) Zhao, Y.; Zuo, S.; Miao, M. The Effect of Oxygen on the Microwave-Assisted Synthesis of Carbon Quantum Dots from Polyethylene Glycol. *RSC Adv.* **2017**, *7*, 16637−16643.

(19) van Dam, B.; Nie, H.; Ju, B.; Marino, E.; Paulusse, J. M. J.; Schall, P.; Li, M.; Dohnalová, K. Excitation-Dependent Photoluminescence from Single-Carbon Dots. *Small* **2017**, *13*, 1702098.

(20) Qu, S.; Zhou, D.; Li, D.; Ji, W.; Jing, P.; Han, D.; Liu, L.; Zeng, H.; Shen, D. Toward Efficient Orange Emissive Carbon Nanodots through Conjugated sp^2-Domain Controlling and Surface Charges Engineering. *Adv. Mater.* **2016**, *28*, 3516−3521.

(21) Miao, X.; Qu, D.; Yang, D.; Nie, B.; Zhao, Y.; Fan, H.; Sun, Z. Synthesis of Carbon Dots with Multiple Color Emission by Controlled Graphitization and Surface Functionalization. *Adv. Mater.* **2018**, *30*, 1704740.

(22) Yuan, F.; Li, S.; Fan, Z.; Meng, X.; Fan, L.; Yang, S. Shining Carbon Dots: Synthesis and Biomedical and Optoelectronic Applications. *Nano Today* **2016**, *11*, 565−586.

(23) Yuan, F.; Yuan, T.; Sui, L.; Wang, Z.; Xi, Z.; Li, Y.; Li, X.; Fan, L.; Tan, Z. a.; Chen, A.; Jin, M.; Yang, S. Engineering Triangular Carbon Quantum Dots with Unprecedented Narrow Bandwidth Emission for Multicolored LEDs. *Nat. Commun.* **2018**, *9*, 2249.

(24) Jia, H.; Wang, Z.; Yuan, T.; Yuan, F.; Li, X.; Li, Y.; Tan, Z. a.; Fan, L.; Yang, S. Electroluminescent Warm White Light-Emitting Diodes Based on Passivation Enabled Bright Red Bandgap Emission Carbon Quantum Dots. *Adv. Sci.* **2019**, *6*, 1900397.

(25) Yuan, F.; He, P.; Xi, Z.; Li, X.; Li, Y.; Zhong, H.; Fan, L.; Yang, S. Highly Efficient and Stable White LEDs Based on Pure Red Narrow Bandwidth Emission Triangular Carbon Quantum Dots for Wide-Color Gamut Backlight Displays. *Nano Res.* **2019**, *12*, 1669−1674.

(26) Ding, H.; Yu, S.-B.; Wei, J.-S.; Xiong, H.-M. Full-Color Light-Emitting Carbon Dots with a Surface-State-Controlled Luminescence Mechanism. *ACS Nano* **2016**, *10*, 484−491.

(27) Tian, Z.; Zhang, X.; Li, D.; Zhou, D.; Jing, P.; Shen, D.; Qu, S.; Zboril, R.; Rogach, A. L. Full-Color Inorganic Carbon Dot Phosphors for White-Light-Emitting Diodes. *Adv. Opt. Mater.* **2017**, *5*, 1700416.

DOI: 10.1021/acs.jpclett.9b01848
J. Phys. Chem. Lett. 2019, 10, 4596−4602

(28) Kwon, W.; Lee, G.; Do, S.; Joo, T.; Rhee, S.-W. Size-Controlled Soft-Template Synthesis of Carbon Nanodots toward Versatile Photoactive Materials. *Small* **2014**, *10*, 506−513.
(29) Peng, H.; Travas-Sejdic, J. Simple Aqueous Solution Route to Luminescent Carbogenic Dots from Carbohydrates. *Chem. Mater.* **2009**, *21*, 5563−5565.
(30) Zhu, S.; Meng, Q.; Wang, L.; Zhang, J.; Song, Y.; Jin, H.; Zhang, K.; Sun, H.; Wang, H.; Yang, B. Highly Photoluminescent Carbon Dots for Multicolor Patterning, Sensors, and Bioimaging. *Angew. Chem., Int. Ed.* **2013**, *52*, 3953−3957.
(31) Zhou, L.; He, B.; Huang, J. Amphibious Fluorescent Carbon Dots: One-Step Green Synthesis and Application for Light-Emitting Polymer Nanocomposites. *Chem. Commun.* **2013**, *49*, 8078−8080.
(32) Sk, M. A.; Ananthanarayanan, A.; Huang, L.; Lim, K. H.; Chen, P. Revealing the Tunable Photoluminescence Properties of Graphene Quantum Dots. *J. Mater. Chem. C* **2014**, *2*, 6954−6960.
(33) Wu, M.; Wang, Y.; Wu, W.; Hu, C.; Wang, X.; Zheng, J.; Li, Z.; Jiang, B.; Qiu, J. Preparation of Functionalized Water-Soluble Photoluminescent Carbon Quantum Dots from Petroleum Coke. *Carbon* **2014**, *78*, 480−489.

NOTE ADDED AFTER ASAP PUBLICATION

This paper published ASAP on July 31, 2019 and reposted on August 6, 2019 with video Supporting Information.

DOI: 10.1021/acs.jpclett.9b01848
J. Phys. Chem. Lett. 2019, 10, 4596−4602